Liquid Crystals
Publication details, including instructions for authors and subscription information:
http://www.informaworld.com/smpp/title~content=t713926090

λ-Shaped mesogens. Structure, phase formation and properties

D. Braun[a]; M. Reubold[a]; L. Schneider[b]; M. Wegmann[a]; J. H. Wendorff[b]
[a] Deutsches Kunststoff-Institut, Darmstadt [b] Fachbereich Physikalische Chemie, Philipps-Universität, Marburg, Germany

To cite this Article Braun, D. , Reubold, M. , Schneider, L. , Wegmann, M. and Wendorff, J. H.(1994) 'λ-Shaped mesogens. Structure, phase formation and properties', Liquid Crystals, 16: 3, 429 — 443
To link to this Article: DOI: 10.1080/02678299408029168
URL: http://dx.doi.org/10.1080/02678299408029168

LIQUID CRYSTALS, 1994, VOL. 16, NO. 3, 429–443

λ-Shaped mesogens

Structure, phase formation and properties

by D. BRAUN, M. REUBOLD, L. SCHNEIDER†, M. WEGMANN and J. H. WENDORFF*†

Deutsches Kunststoff-Institut, Darmstadt

and

†Fachbereich Physikalische Chemie, Philipps-Universität, Marburg, Germany

(*Received 14 June 1993; accepted 11 September 1993*)

This contribution is concerned with molecules composed of rigid linear segments which are connected in such a way that a λ-shape results. Such types of shape have been predicted to lead to an enhanced solubility in low molar mass solvents and in the melt state of flexible chain molecules. The theoretical treatment predicted additionally that such molecules should be able to form lyotropic and thermotropic liquid crystalline phases. Experimental data on the thermodynamic properties, the structure formation in the solid and fluid condensed state, the solubility in low molar mass solvents and selected optical and electro-optical properties are reported; these are in good agreement with the predictions.

1. Introduction

The concept that the structure in the condensed fluid state is primarily controlled by the shape of the molecules dates back to van der Waals [1, 2]. At that time, molecules of nearly spherical symmetric shape, leading to positional short range order in isotroic melts, were considered. This concept was later found to hold also for rod-like molecules which display a strong tendency to form calamitic phases and for disc-like molecules which tend to display discotic phases. Both computer simulations [3] and theoretical considerations such as those based on lattice treatment have emphasized the decisive role of molecular shape in controlling liquid crystalline phase formation [4–6].

However, today, a large number of examples exists which demonstrate that variations—disturbing the ideal rod-like or disc-like shape considerably—can be imposed on the molecules without actually leading to a depression of the formation of calamitic or discotic phases. This is a very favourable situation, since this allows us to control, for a given liquid crystal phase, macroscopic properties such as, for instance, optical, electro-optical, and dielectric properties over a large range by employing a suitably chosen molecular architecture. Examples are provided by chiral smectic C* systems, where the dipole moment must be large along a direction perpendicular to the long axis of the molecule as far as ferroelectric display applications are concerned [7, 8]. Other examples are systems optimized with respect to their solubility by lateral groups, laterally attached flexible side groups etc.

This paper is concerned with a particular shape variation designed for the purpose of reinforcing polymer matrices on a molecular scale, i.e. for molecular

*Author for correspondence.

0267–8292/94 $10·00

reinforcement [9, 10]. The requirements were that the molecules should contain elongated, rigid, linear segments, and that the solubility of such rigid molecules should be as high as possible in polymer matrices.

In order to find molecules consisting of rigid linear segments which, nevertheless, are soluble in common solvents and in particular in matrices composed of flexible chain molecules, we tested various shapes employing lattice calculations [11, 12]. The reason for this choice was that it has been demonstrated in the past that lattice theory is able to account at least qualitatively for the correlations which exist between chemical structure, the shape and flexibility of the molecules on the one hand and their phase behaviour, structure formation and solubility, on the other hand [13–15]. These lattice calculations, which will not be considered in detail here, predicted that rigid star-shaped molecules should be the optimum choice for the purpose of obtaining an enhanced solubility and reinforcement effect. The theory predicted also that molecules having a T-shape and planar variations of this shape such as λ-shaped molecules should also display a better solubility than that given by a corresponding single linear segment. The expectation, based on simulations, is furthermore that such λ-shaped molecules should display liquid crystalline phases. Since it is easier to synthesize λ-shaped molecules as compared to rigid star or ideal T-shaped molecules, we decided to synthesize and characterize such molecules as a first step. The properties to be considered were solubility, the types of phase observed for the condensed state, and the thermal, optical and electro-optical properties.

2. Selection of a suitable chemical structure

The requirements are that linear rigid segments are coupled via a rigid central link in such a way that a planar molecule results. We considered various types of linear segments consisting purely of phenyl units, composed of phenyl units and possessing a OCH_3-end group and, finally, segments composed of phenyl benzoate units, again with various type of end group to be considered later in more detail. Preliminary studies showed that the latter type of segment gives rise to favourable properties of the corresponding λ-type molecules as far as solubility, the location of the transition temperatures and the formation of liquid crystalline phases are concerned. We therefore decided to construct λ-molecules on the basis of such segments. The synthesis is described below. As the trifunctional central link, we selected a 1,2,4-substituted benzene ring (see scheme) and we chose molecules characterized by different values of n and different end groups R (see scheme and table). In the following account, we will represent the various molecules by the symbol λ-m-p, where m represents the number of aromatic rings in the molecule and p the number of carbon atoms in each end group R.

Of course, such structures will not give rise to molecules with an ideal rigidity. In order to get information on the actual shape, particularly at elevated temperatures, we performed computer simulations to obtain the minimum energy conformation for a given temperature, and thus information about shape and rigidity. We performed semi-empirical quantum mechanical calculations [16–18] for this purpose which provided the additional advantage that they were also able to provide information on intrinsic properties such as the dipole moment, the optical polarizibility or simply the length. Such information turned out to be very helpful for the interpretation of the experimentally determined optical properties. The results [19] of such calculations have been published previously [20]. It is sufficient to state here

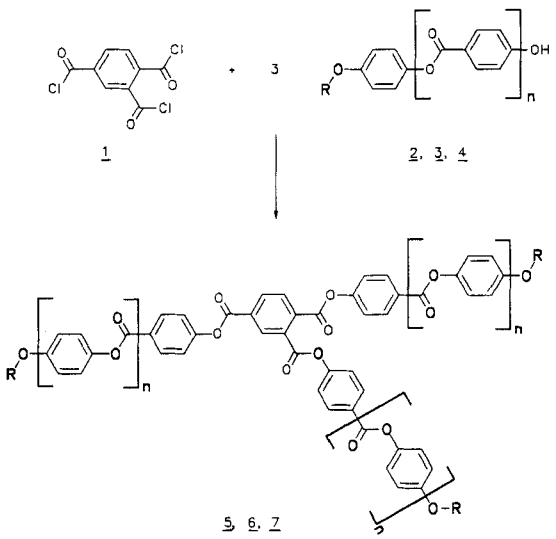

Synthesis of the λ-shaped molecules **5**, **6** and **7** for which $n=1$, 2 and 3, respectively—see the table, where the relationship of the structure numbers (**5**, **6** or **7**) to the code names (based upon number of aromatic rings and the number of carbon atoms in each of the terminal groups *R*) is made clear.

Phase behaviour of λ-type compounds.

Compound	*n*	*R*	Code name	Phase behaviour/°C
5a	1	Methyl	λ-7-1	C 85 S 184 N 258 I
5b	1	Propyl	λ-7-3	C 103 S 173 N 245 I
5c	1	Butyl	λ-7-4	C 105 S 135 N 189 I
5d	1	Hexyl	λ-7-6	C 112 S 150 N 166 I
5e	1	Octyl	λ-7-8	C 108 S 163 N 172 I
5f	1	Dodecyl	λ-7-12	C 84 S 183 N 190 I
6a	2	Methyl	λ-10-1	C 63 S 240 N 318 I
6b	2	Propyl	λ-10-3	C 167 S 208 N 309 I
6c	2	Butyl	λ-10-4	C 172 S 279 N 326 I
7	3	Butyl	λ-13-4	C 144 S 286 N 306 I

that the predicted shape of the molecule, which is shown in figure 1, resembles a λ-shape and that it possesses sufficient rigidity, even at elevated temperatures, to display a geometry distinctively different from that of a rod. This should lead moreover to an enhancement of the solubility compared with that of corresponding materials consisting of rod-like molecules. Further information on the actual shape of such molecules will be given below.

3. Experimental

Thermodynamic properies such as the location of the thermodynamic transition temperatures and the glass transition were characterized using a Perkin-Elmer DSC 4. The heating and cooling rates were 20 K min^{-1}. The electro-optical (Kerr effect) studies were performed with an experimental set-up described previously [21]. The X-ray studies were performed using a Siemens D500 wide angle goniometer and a Kratky compact camera in the small angle regime; CuK_α radiation ($\lambda = 0{\cdot}1542$ nm) was used in all cases, and both set-ups were equipped with thermostatted cells. The optical microscopical studies were done with a Leitz polarizing microscope equipped with a Mettler hot stage.

4. Synthesis

1,2,4-*Benzenetricarbonyl chloride* (**1**) was prepared according to [22]. Yield 75 per cent; b.p. 143°C/3 mmHg [22]: 144–148°C/3 mmHg.

4-Ethoxycarbonyloxybenzoyl chloride was synthesized as already described [23]. Yield 86 per cent; b.p. 132–134°C/1–2 mmHg [23]: 170°C/12 mmHg.

4-Alkoxyphenyl 4-ethoxycarbonyloxybenzoates: 0·15 mol of 4-alkoxyphenol was dissolved in 50 ml of dry methylene chloride and 25 ml of dry triethylamine. The solution was cooled with an ice-bath, and a mixture containing 0·15 mol of 4-ethoxycarbonyloxybenzoyl chloride in 50 ml of dry methylene chloride were added dropwise with vigorous stirring. The reaction mixture was stirred at room temperature for an additional 18 h, and then it was poured into ice/hydrochloric acid to remove the excess of triethylamine. The organic layer was separated and evaporated to give the 4-alkoxyphenyl 4-ethoxycarbonyloxybenzoate which was used for the next step without further purification.

4-Alkoxyphenyl 4-hydroxybenzoates (**2**): 0·1 mol of 4-alkoxyphenyl 4-ethoxycarbonyloxybenzoate was suspended in a mixture of 150 ml of pyridine, 300 ml of acetone, 20 ml of conc. aqueous ammonia solution and 150 ml of water. After stirring at room temperature for 16 h, the suspension was acidified with hydrochloric acid. The precipitate was collected and recrystallized from acetone/water (1:1, v/v) and dried *in vacuo* at 60°C.

2a (R = methyl): Yield 64 per cent; m.p. 195°C,
2b (R = propyl): Yield 76 per cent; m.p. 190°C,
2c (R = butyl): Yield 66 per cent; m.p. 154°C,
2d (R = hexyl): Yield 63 per cent; m.p. 159°C,
2e (R = octyl): Yield 76 per cent; m.p. 155°C,
2f (R = dodecyl): Yield 43 per cent; m.p. 143°C.

4-(4-Alkoxyphenyloxycarbonyl)phenyl 4-hydroxybenzoates (**3**) were prepared from 4-alkoxyphenyl 4-hydroxybenzoates (**2**) and 4-ethoxycarbonyloxybenzoyl chloride according to the above procedure:

3a (R = methyl): Yield 37 per cent; m.p. 187°C
3b (R = propyl): Yield 63 per cent; m.p. 178°C,
3c (R = butyl): Yield 47 per cent; m.p. 144°C.

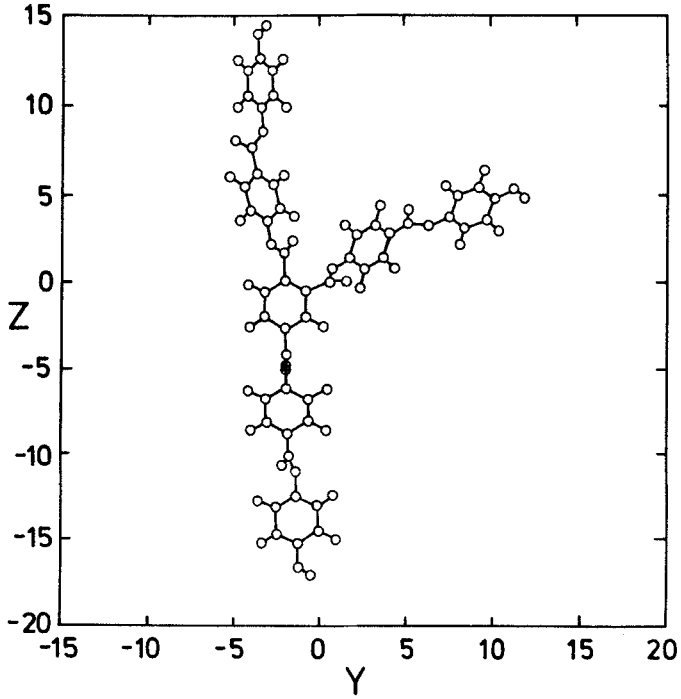

Figure 1. Results of MNDO calculations on the shape of the mesogens as illustrated for λ-7-1.

4-[4-(4-Butoxyphenyloxycarbonyl)phenyloxycarbonyl]phenyl 4-hydroxybenzoate (**4**) was prepared from 4-(4-butoxyphenyloxycarbonyl)phenyl 4-hydroxybenzoate (**3c**) and 4-ethoxycarbonyloxybenzoyl chloride according to the above procedure. Yield 61 per cent; m.p. 123–126°C.

1,2,4-Benzenetricarboxylates (**5**, **6**, **7**) were prepared from **2**, **3** and **4**, resp., together with **1** according to a procedure similar to that described earlier. The raw materials obtained were flash chromatographed over silica gel using trichloromethane/isopropyl alcohol (10:1, v/v) as eluent to give **5**, **6** and **7**, respectively.

5. Thermodynamic properties

5.1. *Solubility and lyotropic phase behaviour*

One prediction of the lattice treatment was that the solubility of the λ-type molecules should be much better than that found for the linear segments of which the λ-shaped molecules are composed. This is in agreement with the experimental results: ethanol, acetone, dichloromethane, THF and mixtures of trichloromethane with isopropyl alcohol were used as solvents. The solubility decreases, as expected, with increasing length of the rigid linear segments.

In addition, the lattice treatment predicted that the λ-type molecules are able to form a lyotropic liquid crystalline phase. Again this is in agreement with experimental results; we observed a nematic schlieren texture for solutions of such compounds in, for instance, dichloromethane. A biphasic concentration range extending between 65 and 83 wt per cent of the 1-7-4 mesogen was observed, for instance.

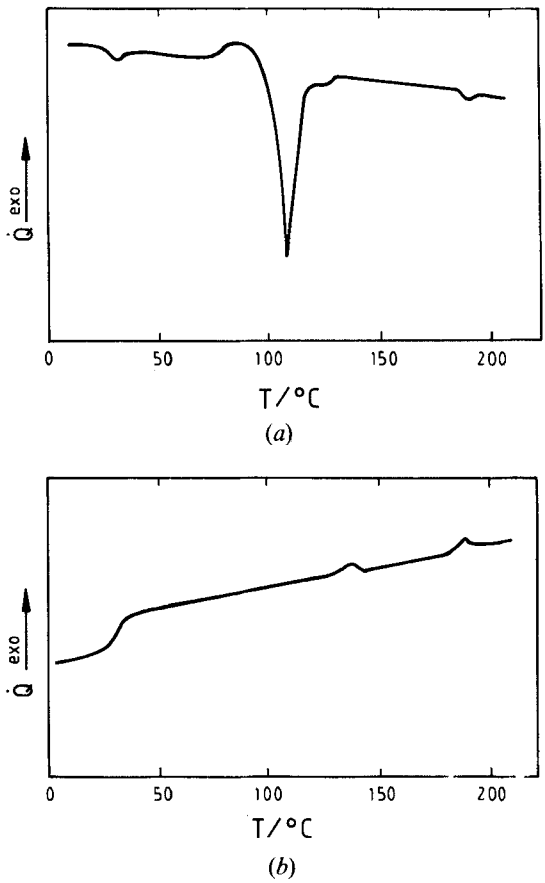

Figure 2. DSC runs: (*a*) heating, (*b*) cooling (sample: λ-7-4).

5.2. *Thermodynamic transitions in the condensed state*

Next we will consider the results obtained for the phase behaviour in the condensed state (see table). A detailed discussion will only be given for the molecule λ-7-4. Figure 2(*a*) shows a DSC run obtained on heating for a sample cast from solution. The solution cast material is crystalline and melts at a temperature of 105°C (detailed data showing that the solution cast material is really crystalline are later given in terms of X-ray results). The DSC trace further reveals two additional, but much weaker transitions, which can be attributed—based on X-ray and optical studies to be reported below—to a transition from a smectic A to a nematic (at a temperature of 135°C) and from a nematic to an isotropic state at a temperature of 189°C. These latter two transitions are reversible, as is apparent from the cooling curve shown in figure 2(*b*). A peculiar feature seems to be the fact that the smectic nematic transition occurs at a higher temperature on the cooling run, compared to the heating run. It has, however, to be pointed out that the sample used for the first heat was obtained from solution and may still contain some traces of solvent. Drying at sufficiently elevated temperatures was not performed in order not to destroy the well-developed original crystalline state.

The crystalline state is strongly suppressed on cooling from the melt, and the smectic A phase is transformed into the corresponding glassy state. The glass transition is connected with a stepwise decrease of the specific heat (see figure 2 (*b*)). Slow heating of the glassy state causes the material to crystallize again at temperatures well above the glass transition and well below the melting point of the crystalline state. Such a behaviour is not unusual both for low molar mass and polymeric liquid crystal materials; the suppression of crystallization is a purely kinetic phenomenon.

Similar results were obtained for the other λ-type materials considered. The results obtained from the DSC studies, which are displayed in the table, are manifestations of the effect of the length of the rigid segments and of the flexible end groups on the transition behaviour. The transition temperatures tend to increase with the length of the rigid segments but not always consistently. The transition temperatures depend furthermore on the type of end group, yet there is again no regular variation with the length of this alkoxy group. The effect of the length of the segments and end groups on the solubility is more consistent and much stronger.

6. The phases displayed in the condensed state

6.1. *The crystalline state*

The λ-molecules considered here display a crystalline state if obtained from solution. This is quite apparent from the X-ray diagram displaying a large number of sharp reflections both in the small and wide angle regime (see figure 3). In the following, we will, for the sake of simplicity, discuss in more detail the results obtained for just one particular λ-molecule, λ-7-4. The analysis of the X-ray results shows that this system displays an orthorhombic cell with the dimensions $a = 0{\cdot}543$ nm, $b = 2{\cdot}460$ nm, and $c = 3{\cdot}965$ nm. The *c*-dimension corresponds very well with the length along the principal axis predicted by the MNDO calculations. This length scale is roughly the same as the one observed for the smetic A phase to be considered below. The *b*- and *a*-dimensions correspond in order of magnitude to the two length scales perpendicular to the principal axis. Based on packing considerations, we propose a model which is able to account for all the experimental facts available to us.

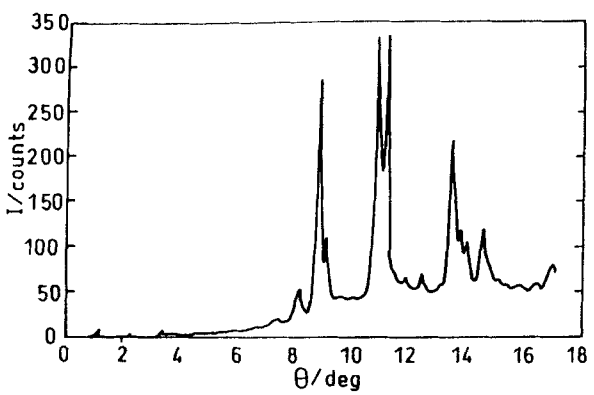

Figure 3. X-ray results obtained for the crystalline state (sample: λ-7-4).

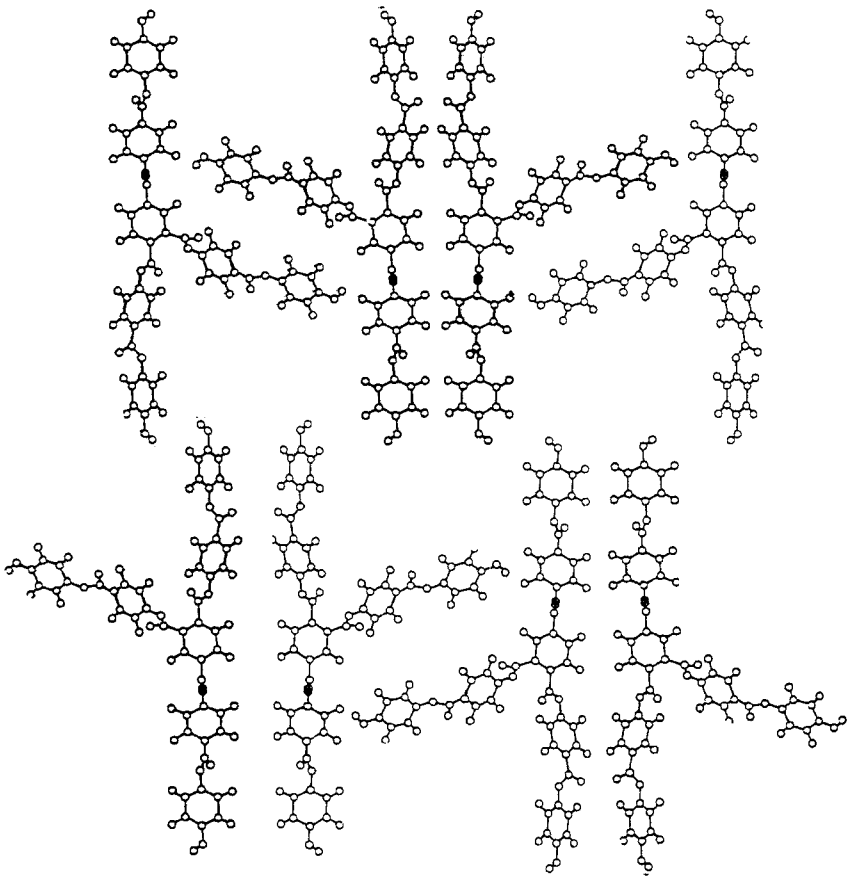

Figure 4. Model for the packing in the crystalline state.

The proposal is that pairs of λ-molecules are arranged antiparallel, as shown in figure 4 and that such pairs are arranged on the nodes of the lattice and at the base of the cell (base centred). The b-dimension fits exactly with the value predicted by MNDO calculation for the antiparallel packing of the rigid λ-molecules. The a-dimension is close to the values found for linear segments with the corresponding chemical structure [24]. It should be pointed out that such an antiparallel packing was also predicted to occur by Monte Carlo simulations performed in two dimensions [25].

The volume of the unit cell thus amounts to 5296·37 Å^3; the number of molecules in the cell is $N=4$. The theoretically obtained density is

$$\rho_{\text{theor}} = 1{\cdot}274\ \text{g cm}^{-3}$$

as compared to the experimental value:

$$\rho_{\text{exp}} = 1{\cdot}238\ \text{g cm}^{-3}.$$

6.2. *The smectic phase*

The smectic phase is characterized by a layer structure (see figure 5); the periodicity is slightly lower than that found for the crystalline state. One of the

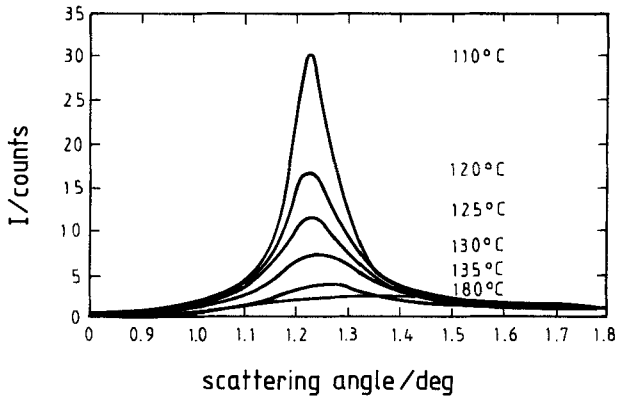

Figure 5. X-ray results obtained for the smectic phase and the nematic phase as the temperature is changed (sample: λ-7-4).

reasons for such a decrease is certainly the onset of conformational disorder in the flexible end groups. Such a decrease of the linear dimension at the transition from the crystalline is the smetic phase is a general phenomenon. A broad halo is observed in the wide angle scattering indicating the presence of a short range order within the layers. Therefore the conclusion is that the λ-7-4 molecules display a smectic A phase.

The mean distance obtained from the location of the halo corresponds to the '*a*'-dimension observed for the crystalline state. In combination with the value obtained for the layer distance, we expect that the local packing within the smectic layer is controlled again by the antiparallel pairs of molecules which constitute the motif in the crystalline state. We will later discuss further results which are consistent with this proposal. Such a packing gives rise locally to a biaxial packing, but conoscopic studies performed on samples with a homeotropic texture show beyond any doubt that no macroscopic biaxial symmetry exists [19], and that the sample is uniaxial, as expected for a smectic A phase.

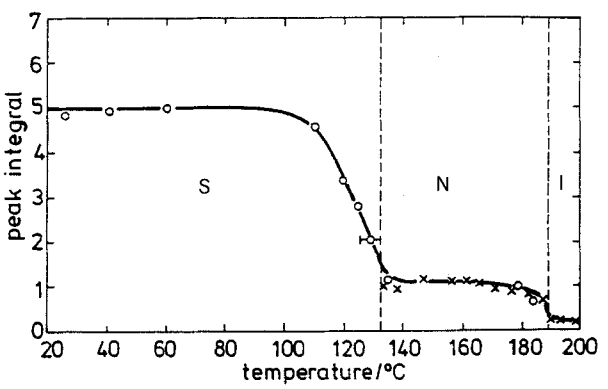

Figure 6. Variation of the small angle reflection intensity with temperature in the nematic and smectic phase (sample: λ-7-4).

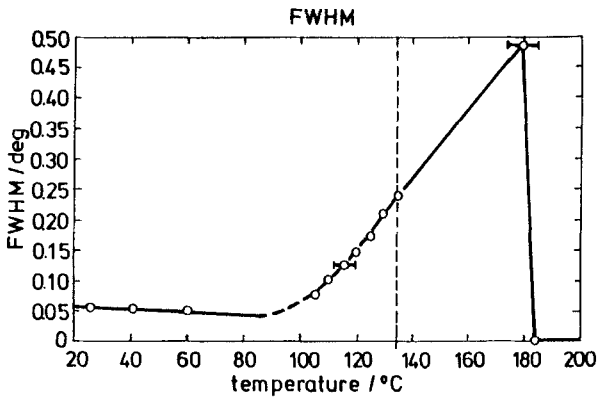

Figure 7. Variation of the width of the small angle reflection with temperature in the nematic and smectic phase (sample: λ-7-4).

An interesting feature is the dependence of the scattering intensity characteristic of the small angle peak on the temperature. The intensity is approximately constant below about 110°C, yet above this temperature it decreases quite strongly with increasing temperature. In addition one finds that the width of the reflection increases strongly with increasing temperature (see figure 5, 6 and 7).

The features described so far are qualitatively characteristic of second order phase transitions i.e. continuous variations of the spatial correlations. According to theory, the smectic A–nematic transition may be of second order [26, 27]. The features mentioned above may, however, also occur for a transition which is weakly first order: the presence of a small transition peak in the DSC diagram points to a first order transition. Therefore, the conclusion based on the X-ray and DSC results is that the transition from the smectic phase to the nematic phase is first order, but weakly first order.

6.3. *The nematic phase*

Polarizing microscopic observations indicate that the higher temperature fluid state corresponds to a liquid crystalline nematic phase, as apparent from the observed birefringence and the characteristic schlieren texture.

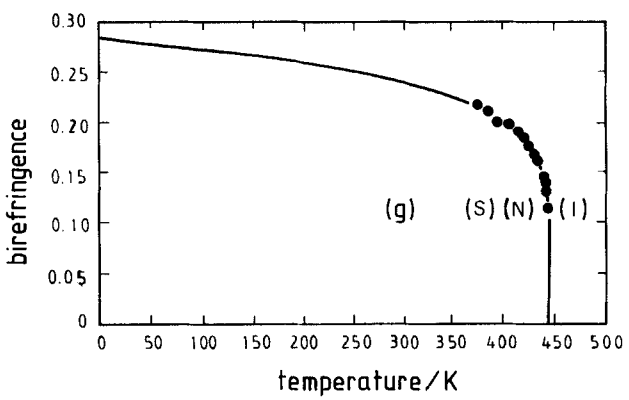

Figure 8. Variation of the birefringence with temperature (samle: λ-7-4).

The nematic melt displays two weak halos in the wide and small angle regime, respectively, in the temperature range close to the transition into the isotropic state. The halos become just slightly more distinct as the sample is cooled down. Based on the observation of a nearly continuous transition between the nematic and the smectic A phase and based on optical studies to be described later, we assume that the local packing is still the same as in the smectic phase, as described above. To test this assumption, we carried out experiments on the birefringence within the smectic and nematic phases and performed corresponding MNDO calculations. The analysis of these optical results, in combination with the results of the MNDO calculations, allows us to draw conclusions in this respect.

Experimental results were obtained for the smectic and nematic phases by measuring the refractive index parallel and perpendicular to the director for a macroscopically oriented sample, using a wave guide method [19, 20]. The results are displayed in figure 8. To obtain values for the birefringence corresponding to an order parameter of $S=1$, we used two approaches. In the first, we used an extrapolation often used in the literature [28]:

$$\Delta n(T)=\Delta n(S=1)(1-T/T_{NI})^b$$

where T_{NI} is the nematic–isotropic transition temperature.

This extrapolation is shown in figure 8. The extrapolated value turned out to be

$$\Delta n(S=1)=0{\cdot}28\pm0{\cdot}05;\quad S(22^\circ C)=0{\cdot}8;\quad b=0{\cdot}15.$$

In a second approach we dissolved 1 wt per cent of azobenzene in λ-7-4 and measured the order parameter using UV-dichroism. The result obtained in this case for the birefringence

$$\Delta n(S=1)=0{\cdot}25\pm0{\cdot}03$$

is in good agreement with that obtained by extrapolation.

These results have now to be compared with those obtained by the theoretical analysis. The MNDO results on the polarizibility tensor for a single λ-7-4 molecule [19, 20] are:

$$a=\begin{pmatrix}35{\cdot}6 & 0 & 0\\ 0 & 81{\cdot}6 & 1\\ 0 & 0 & 109{\cdot}3\end{pmatrix}\times10^{-40}\,\mathrm{F\,m}.$$

The largest polarizability is observed within the YZ-plane containing the main axis and the branch. Using these values, we can calculate the expected values for the refractive index parallel and perpendicular to the director for the particular case of an order parameter $S=1$, and also for the corresponding birefringence as follows [28]:

$$(n_i^2-1)/(n^2+2)=N\alpha_i/3e_o$$

with i = parallel/perpendicular and where N is the particle density, $N=7{\cdot}345\times10^{26}\,\mathrm{m}^{-3}$. Assuming that the λ-molecule has the shape displayed in figure 1 and that a random orientational arrangement of the side branches about the main axis

occurs at least on a macroscopic scale, the result turned out to be

$$\Delta n(S=1)=0{\cdot}242$$

Predictions and experimental results therefore agree closely for the case that the λ-molecule is assumed to have the shape displayed in figure 1 and that a random orientational arrangement about the main axis exists on a macroscopic scale (uniaxial symmetry). If we assume that all branches of the λ-molecules are parallel to the director (distorted molecule), we obtain predicted values which are much too high compared with the experimentally obtained values.

6.4. *The isotropic state and its pretransitional behaviour*

The isotropic melt is characterized in terms of X-ray scattering by just a prominent halo in the wide angle regime and by a very weak halo at small angles. This characteristic pattern is not significantly changed at the transition into the nematic phase. The halos are apparently connected with the short range order along and perpendicular to two principal axes of the molecules (see below for discussion).

The isotropic phase is expected to display pretransitional effects, since the isotropic—nematic transition is known to be weakly first order and to display such pretransitional phenomena. One convenient way to characterize these pretransitional properties consists in the analysis of the electro-optical Kerr constant B in the isotropic phase in the vicinity of the N–I transition. The Landau–de Gennes treatment of such pretransitional effects leads to the following expression for the Kerr constant B [29]:

$$B=\Delta n^0\Delta\varepsilon^0\varepsilon_0/3\lambda a_0(T-T^*)$$

(Δn^0 and $\Delta\varepsilon^0$ are saturation values ($S=1$) for the anisotropy of the polarizibility and the dielectric constant, respectively; a_0 is the expansion coefficient of the Landau–de Gennes expansion of the free energy) where the characteristic temperature T^* is typically 1 K below the actual first order phase transition T_{NI}. Figure 9 displays the results obtained from the Kerr studies. The Kerr constant B is plotted as a function of the temperature. The divergence at lower temperature is quite apparent. A plot of the inverse of the Kerr constant versus the temperature leads to a straight line, which

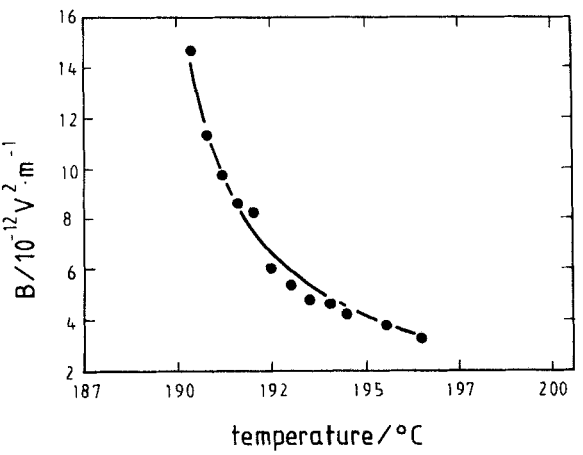

Figure 9. Results of Kerr effect studies (sample: λ-7-4).

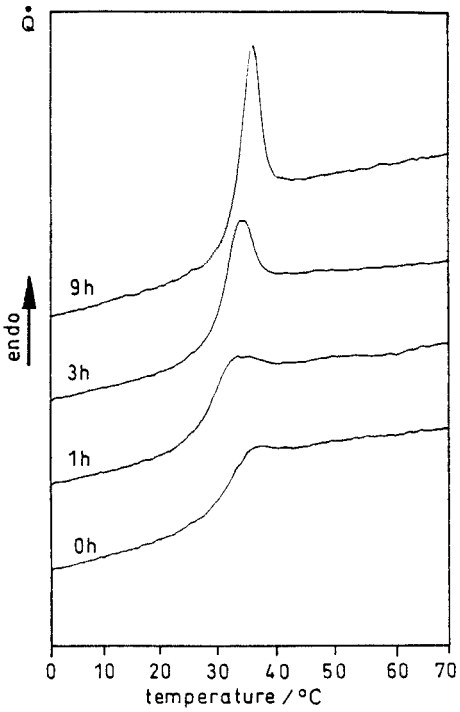

Figure 10. Enthalpy relaxation in the smectic A glass as obtained by DSC (sample: λ-7-4).

allows one to obtain the characteristic temperature T^*. It actually turns out to be about 1 K below the clearing temperature.

The data obtained from the Kerr studies and the thermodynamic studies allow conclusions to be drawn about the value of the correlation parameter g_2, which corresponds to the number of molecules which are orientationally correlated in the

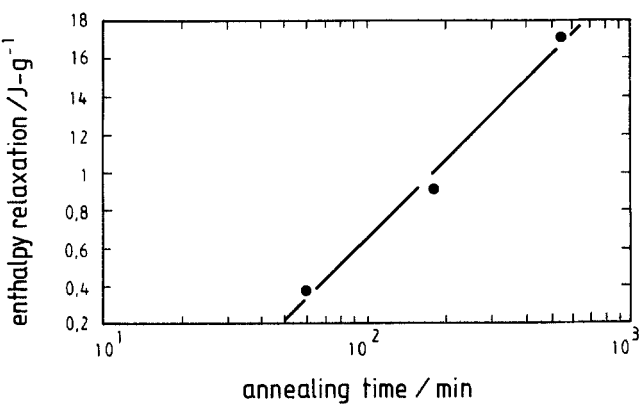

Figure 11. Rate of enthalpy relaxation in the smectic A glass as obtained by DSC (sample; λ-7-4).

fluid state. Theory predicts [30]

$$g_2 = (45NkT)/(n^2+2)a_0(T-T^*).$$

The analysis leads to the conclusion that about 200 molecules are orientationally correlated at a temperature surpassing T^* by 1 K. This is about the number observed for many other calamitic systems [30]. So, in this respect the λ-molecules behave like any other calamitic system.

6.5. *The glassy smectic A state*

Finally, we will consider the glassy smectic state. The presence of such a state with a glass transition temperature well above room temperature allows us to prepare solid films having the structural and optical properties of the smectic phase. In the following, we will describe results of investigations concerned with the characteristic properties of glasses in general. The structure found for the glassy state corresponds of course to that of the equilibrium fluid smectic state. The transition into the glassy state is connected, as pointed out above, with a stepwise decrease of the specific heat, the magnitude of which is characteristic of amorphous organic glases and also for many disordered liquid crystalline glasses [31]: glasses formed within higher ordered liquid crystalline phases show a tendency to display vanishing changes of the specific heat at the glass transition, which makes the calorimetric detection of the glass transition difficult.

A particular feature of the glassy state originating from its non-equilibrium state is its ageing behaviour. The ageing process can be considered as a manifestation of the thermodynamic non-equilibrium nature of the glassy state: it tends, by slow relaxation, to approach the equilibrium state corresponding to the supercooled melt [32, 33]. Ageing is thus connected, among others, with the relaxation of the volume and the enthalpy, the enthalpy relaxation leading to an endotherm on heating, superimposed on the stepwise change of the specific heat characteristic of unaged materials. Figure 10 displays such peaks for λ-7-4. The analysis of the ageing time dependence of the peak height allows one to obtain information on the characteristic ageing time

$$r = d((\Delta H(t))/d(\ln t) = 0{\cdot}61.$$

Figure 11 shows the values obtained for λ-7-4. The values are obtained for a reference undercooling of 10 K. The values are well within the range observed for low molar mass liquid crystalline systems and quite different from the values observed for amorphous polymeric glasses, for instance.

7. Conclusions

The conclusion first of all is that a modification of a rigid linear molecule leading to a λ-shaped molecule does not affect the tendency to form calamitic liquid crystalline phases. The shape variation does control, however, properties such as melting, glass formation and, in particular, solubility. We have not discussed in this contribution the effect of molecules of such shape on the mechanical properties of blends with flexible chain polymers. It is sufficient to state here that we could actually demonstrate a strong molecular reinforcement effect [34].

We would like to thank the Deutsche Forschungsgemeinschaft (DFG) for financial support.

References

[1] KOHLER, F., 1972, *The Liquid State* (Verlag Chemie), p. 21.
[2] EGELSTAFF, P. A., 1967, *An Introduction to the Liquid State* (Academic Press), p. 12.
[3] ALLEN, M. P., and WILSON, M. R., 1989, *J. Comput. Aid. Molec. Design*, **3,** 335.
[4] FLORY, P. J., 1984, *Adv. Polym. Sci.*, **59,** 1.
[5] FLORY, P. J., 1956, *Proc. R. Soc.* A, **234,** 73.
[6] DE GENNES, P. G., 1974, *The Physics of Liquid Crystals* (Clarendon Press, Oxford), p. 1.
[7] POTS, H., SCHÖNFELD, A., ZENTEL, R., KREMER, F., and SIEMENSMEYER, K., 1992, *Adv. Mater.*, **4,** 351.
[8] WALBA, D. M., RAVAZI, H. A., HORIUCHI, A., EIDMAN, K. F., OTTERHOLM, B., HALTIWANGER, R. C., CLARK, N. A., SHAO, R., PARMAR, D. S., WAND, M. D., and VOHRA, R. T., 1991, *Ferroelectrics*, **113,** 21.
[9] TAKAYANAGI, M., 1983, *Pure appl. Chem.*, **55,** 819.
[10] BORSTOW, W., 1988, *Kunststoffe*, **78,** 411.
[11] GALLENKAMP, U., 1989, Ph.D. Thesis, Darmstadt.
[12] CLAßEN, S., GALLENKAMP, U., WOLF, M., and WENDORFF, J. H., 1989, *Integration of Fundamental Polymer Science and Technology*, Vol. IV, edited by P. Leemstra (Elsevier), p. 232.
[13] FLORY, P. J., 1971, *Principles of Polymer Chemistry* (Cornell University Press), p. 1.
[14] BALLAUFF, M., 1986, *Macromolecules*, **9,** 1366.
[15] ERMAN, B., FLORY, P. J., and HUMMEL, J. P., 1980, *Macromolecules*, **13,** 484.
[16] STEWART, J. J. P., 1990, *J. Comput. Aid. Molec. Design*, **4,** 1.
[17] CLARK, T. A., 1985, *A Handbook of Computational Chemistry* (J. Wiley), p. 1.
[18] STEWART, J. J. P., 1988, *New polym. Mater.*, **1,** 53.
[19] WEGMANN, M., 1989, Master Thesis, Darmstadt. REUBOLD, M., 1989, Master Thesis, Darmstadt.
[20] BRAUN, D., REUBOLD, M., WEGMANN, M., and WENDORFF, J. H., 1991, *Makromolek Chem. rap. Comun.*, **12,** 151.
[21] ULLRICH, K. H., and WENDORFF, J. H., 1985, *Molec. Crystals liq. Crystals*, **313,** 361.
[22] DRECHSLER, G., and HEIDENREICH, S., 1965, *J. prakt. Chem.*, **27,** 163.
[23] FISCHER, E., and FREUDENBERG, K., 1910, *Justus Liebigs Annln Chem.*, **372,** 32.
[24] ZIMMERMANN, H., 1987, Thesis, Darmstadt.
[25] SEIFERT, A., SCHARTEL, B., and WENDORFF, J. H.., 1993, Poster presented at the Makromolekulares Kolloquium, Freiberg.
[26] LUBENSKY, T. C., 1983, *J. Chim. phys.*, 8031.
[27] DAVIDOV, D., SAFINYA, C. R., KAPLAN, M., DANA, S. S., SCHAETZING, R., BIRGENEAU, B. J., and LITSTER, J. D., 1979, *Phys. Rev.* B, **19,** 1657.
[28] DE JEU, W. H., 1979, *Physical Properties of Liquid Crystalline Materials* (Gordon and Breach Sci., New York), p. 11.
[29] BIRENHEIDE, R., BUDESHEIM, K. W., and WENDORFF, J. H., 1991, *Angew. Makromolek. Chem.*, **185,** 319.
[30] FINKELMANN, H., BENTHACK, H., and REHAGE, G., 1982, *J. Chim. phys.*, 35.
[31] STRUIK, L. C. E., 1978, *Physical Aging in Amorphous Materials and Other Materials* (Elsevier), p. 1.
[32] KOVACS, A. J., HUTCHINSON, J. M., AKLONIS, J. J., and RAMON, A. R., 1979, *J. polym. Sci.*, **7,** 1097.
[33] WUNDERLICH, B., and GREBOWICZ, J., 1984, *Adv. polym. Sci.*, **60, 61,** 1.
[34] BRAUN, B., HARTIG, C., REUBOLD, M., and WENDORFF, J. H., 1993, *Makromolek. chem. rap. Commun.*, **14,** 663.